JOURNAL OF THERMOPHYSICS AND HEAT TRANSFER
Vol. 9. No. 2, April–June 1995

Technical Notes

TECHNICAL NOTES are short manuscripts describing new developments or important results of a preliminary nature. These Notes cannot exceed 6 manuscript pages and 3 figures; a page of text may be substituted for a figure and vice versa. After informal review by the editors, they may be published within a few months of the date of receipt. Style requirements are the same as for regular contributions (see inside back cover).

Modeling of Heat Transfer Processes at Catalytic Materials in Shock Tube

Vladimir V. Riabov*
Worcester Polytechnic Institute, Worcester, Massachusetts 01609
and
Victor P. Provotorov†
Central Aerohydrodynamics Institute (TsAGI), Zhukovsky-3, Moscow 140160, Russia

Introduction

SHOCK tubes have become widely used to study thermodynamic processes in high-temperature gas flows[1] and chemical kinetics.[1] Flow parameters behind incident and reflected shock waves were analyzed by Gaydon and Hurle,[1] Bazhenova et al.,[2] Sturtevant and Slachmuylders,[3] Goldsworthy,[6] Johannesen et al.,[7] and Hanson et al.[8] It was found that the gas behind the reflected shock wave is practically at rest in the laboratory coordinate system, and the temperature in this area is approximately twice as high as behind the incident shock wave. The purpose of the present study is to analyze heat transfer processes at the catalytic materials of the shock-tube end after shock wave refraction in terms of the model of the nonsteady-state nonequilibrium thermal boundary layer, which was developed by Provotorov and Riabov." The previous analysis" has covered the time interval from 10^{-9} s to 2.5 μs, and it was restricted by the applied numerical method. In the present study we have developed the numerical algorithm and studied the gasdynamic parameters, as well as component concentrations in the layer for the time interval up to 100 μs. The parameters behind the reflected shock wave[1] ^{9} were evaluated as the external boundary conditions for the layer. The nonequilibrium parameters in this area are the functions of initial parameters such as pressure and temperature in the shock-tube channel, velocity of the incident shock wave. etc. The dissociation, recombination, and exchange reactions[1] among the major air components (O_2, O. NO, N_2, and N) were considered. At the shock-tube end a union boundary condition[5-9] for temperature and heat flux was used. as well as a boundary condition for recombination of atomic components. Unfortunately, the identical experimental data are unknown to the authors.

Received March 14, 1994; presented as Paper 94-2071 at the AIAA/ASME 6th Joint Thermophysics and Heat Transfer Conference. Colorado Springs. CO, June 20–23, 1994; revision received Aug. 26. 1994; accepted lor publication Sept. 30, 1994.

*Visiting Associate Professor, Department of Mechanical Engineering. Member AIAA.
†Senior Research Scientist. Rarefied Gas Dynamics Branch, Aerothermodynamics Division.

Gas Flow Parameters Behind the Reflected Shock Wave

We have considered the simplest model[1] of the one-dimensional flow behind the incident shock wave, which propagated in an ideal gas with parameters of pressure p_1 = 1 and 100 Pa, and temperature T_1 = 295 K at constant velocity U_S = 5 km/s. The reflected shock wave is propagated in the disturbed field after the incident shock wave.[7,8]

The algorithm of calculation of the parameters behind the incident and reflected shock waves is described by Provotorov and Riabov" in detail. The system of algebraic-differential equations" has been solved at each point of the flowfield behind the incident shock wave under the assumption that air is not dissociated on the shock wave front. A modified Newton's method"[1] with optimal choice of iteration step was used for numerical solution of the equations.

The velocity of the reflected shock wave U_R as a function of time. for two cases of pressure p_1 = 1 and 100 Pa. is plotted in Fig. 1 (squares and triangles, correspondingly). The decrease of the values U_R indicates the nonequilibrium type of chemical reactions behind the incident shock wave.[8] The magnitude of pressure p_1 defines the time required for attainment of the steady-state distribution. And this time is less by approximately a factor of 100 for the case of p_1 = 100 Pa. From this point of view, the parameter U_R is very convenient for experimental verification of the nonequilibrium parameters in the areas behind the shock and near the end of the tube.

Using the technique developed by Provotorov and Riabov," the distribution of temperature T_3 and pressure p_3 behind the reflected shock wave was calculated. The computational technique was used as the same one that was discussed above for the case of the incident shock wave. The computational results are shown in Figs. 2 and 3 for the same cases of the initial pressure p_1. The distribution of temperature T_3 (see Fig. 2) is similar to the distribution of the velocity U_R of the reflected shock wave and it can be useful for the identification of the type of the chemical processes behind the shocks.[7,8] The val-

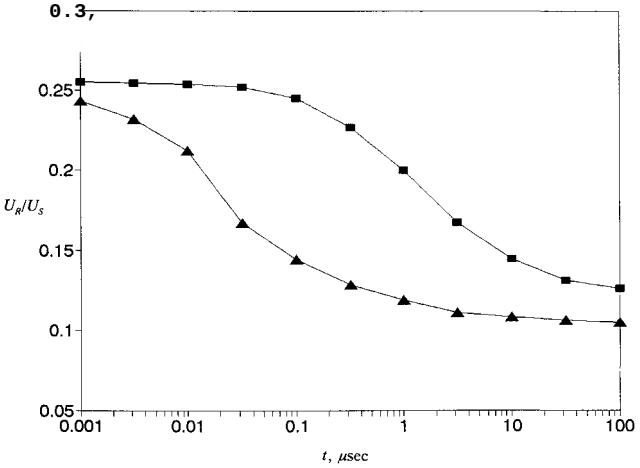

Fig. 1 Velocity of the reflected shock wave U_R as a function of time (■, p_1 = 1 Pa; ▲, p_1 = 100 Pa).

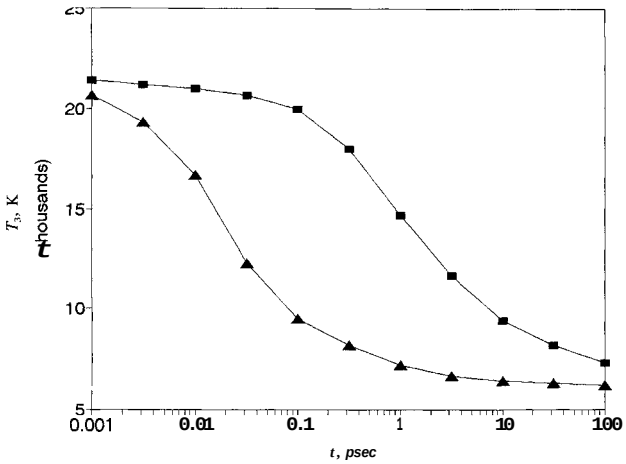

Fig. 2 Temperature T_3 behind the retlected shock wave as a function of time (■, p_1 = 1 Pa; ▲, p_1 = 100 Pa).

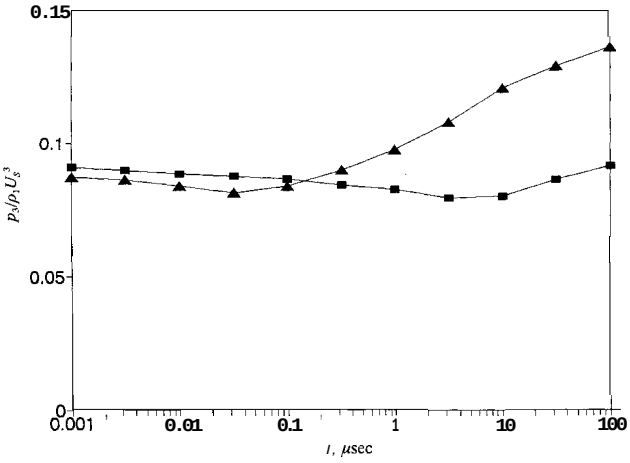

Fig. 3 Pressure p_3 behind the reflected shock wave (and at the tube end) as a function of time (■, p_1 = 1 Pa; ▲, p_1 = 100 Pa).

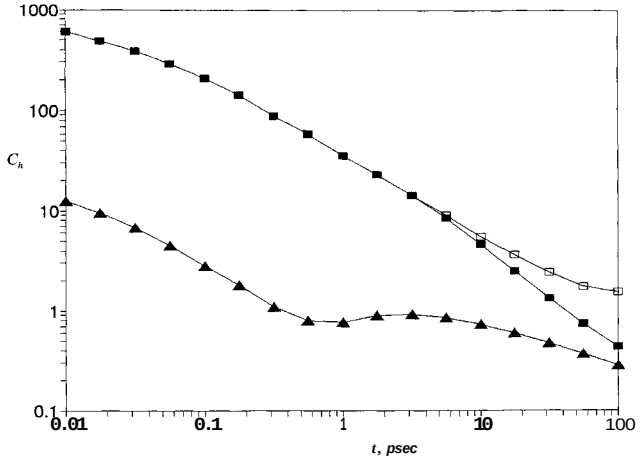

Fig. 4 Heat transfer coefficient C_h at the end wall of the shock tube (■, p_1 = 1 Pa, nickel; ▲, p_1 = 100 Pa, nickel; □, p_1 = 1 Pa, Pyrex).

ues of temperature $T_3(t)$ were used as the external ("outer") boundary conditions for temperature in the thermal viscous layer near the tube end.

Figure 3 presents the computational results for pressure p_3 behind the reflected shock wave as a function of time. This parameter is the most conservative one. Nevertheless, for the case of the large value of initial pressure p_1 = 100 Pa (triangles), the significant increase of the values p_3 is observed after the short initial time-interval of decreasing. This is a result of the influence of different types of chemical relaxation processes behind the incident wave with initial pressure p_1.[5-9] The initial decrease of p_3 is explained by rapid chemical relaxation behind the reflected shock wave.[8] As presented in Fig. 2, the temperature distribution $T_3(t)$ indicates this type of chemical process in the region. In the case p_1 = 100 Pa, the flow behind the reflected shock wave is very close to a state of local thermodynamic equilibrium,' while in the other case p_1 = 1 Pa, the flow is significantly in nonequilibrium.[8,9] The function $p_3(t)$ can be used for the prediction of pressure in the thermal viscous layer near the tube end, and it correlates with the value of pressure $p_w(t)$ at the tube end.

Additional important information is the distribution of the air components behind the reflected shock wave.[9] This data should be used as external boundary conditions for the component concentrations in the thermal viscous layer under the considered conditions.

Heat Flux at the Catalytic Wall

Behind the reflected shock wave the thermal viscous layer begins to grow near the tube end.[5,6] The acceptable model of a nonsteady-state nonequilibrium thermal boundary layer[6,9] could be considered in this area. The system of the thermal boundary-layer equations was analyzed by Provotorov and Riabov" in detail.

A finite difference approximation to the boundary-layer equations, with boundary conditions mentioned above, was constructed analogous to the method using a matrix variant of Keller's two-point "box scheme."[11,12] The spatial and time variables were approximated by the second-order terms. The finite difference stability analysis has been performed by Denisenko and Provotorov" in terms of the spectral method. The two-point difference equations were solved by the matrix regularization technique of Provotorov.[12]

The calculated values of heat transfer coefficient $C_h = q/(\rho_1 U_S^3)$ are shown in Fig. 4 for the range of time $t = 10^{-9}$–10^{-4} s and initial pressure p_1 = 1 and 100 Pa (triangles and squares, correspondingly).

At t < 1 μs the heat flux values differ by a factor of 50. At t > 10 μs this difference is less significant. Although the thermal layer state approaches equilibrium at p_1 = 100 Pa, for the case of initial pressure p_1 = 1 Pa, processes within the thermal layer are of a strongly nonequilibrium character. For this case, the influence of catalytic properties of the wall material is significant. For different catalytic materials (see Fig. 4; empty squares for Pyrex®, filled squares for nickel) the values of heat transfer coefficient C_h differ by a factor of 6 at $t > 30$ μs. This phenomena can be applied to the identification of catalytic properties of heat protection materials.

Concluding Remarks

A method based on the numerical analysis of the thermal viscous boundary layer near the shock-tube end has been developed for studying heat transfer properties of catalytic materials at high temperatures. The dependence of heat flux and pressure at the shock-tube end as well as reflected shock wave velocity upon time provide valuable information on the characteristics of the thermal boundary layer near the tube end and parameters of catalytic wall materials.

The major analysis has been made in terms of one-dimensional nonsteady flow models. In future studies the possible effects of the boundary layers on the tube sidewall should be taken into consideration. However, the problem of an interaction between the sidewall boundary layers with the thermal boundary layer at the shock-tube end wall would require a three-dimensional analysis for a correct interpretation of future experimental results.

References

'Gaydon, A. G., and Hurle, I. R., *The Shock Tube in High-Temperature Chemical Physics,* Reinhold, New York, 1963.

'Bazhenova, T. V., Gvozdeva, L. G., and Lobastov, Yu. G., *Shock Waves in Real Gases,* Nauka, Moscow, Russia, 1968 (in Russian).

'Slack, M. W., "Kinetics and Thermodynamics of the CN Molecule. 3. Shock Tube Measurements of CN Dissociation Rates," *Journal of Chemical Physics,* Vol. 64, No. 1, 1976, pp. 228–236.

'Park, C., Howe, J. T., Jaffe, R. L., and Candler, G., "Review of Chemical-Kinetic Problems of Future NASA Missions, II: Mars Entries," *Journal of Thermophysics and Heat Trunsfer,* Vol. 8, No. 1. 1994. pp. 9–23.

[5]Sturtevant, B., and Slachmuylders, E., "End Wall Heat-Transfer Effects on the Trajectory of a Reflected Shock Wave," *Physics of Fluids,* Vol. 7, No. 8, 1964, pp. 1201–1207.

"Goldsworthy, F. A., "The Structure of a Contact Region, with Application to the Reflection of a Shock from a Heat-Conducting Wall." *Journal of Fluid Mechanics,* Vol. 5, Pt. 1, 1959, pp. 164–176.

[7]Johannesen, N. H., Bird, G. A., and Zienkiewicz, H. K., "Theoretical and Experimental Investigations of the Reflexion of Normal Shock Waves with Vibrational Relaxation," *Journal of Fluid Mechanics,* Vol. 30, Pt. 1, 1967, pp. 51–64.

[8]Hanson, R. K., Presley, L. L., and Williams, E. V., "Numerical Solutions of Several Reflected Shock-Wave Flow Fields with Nonequilibrium Chemical Reactions," NASA TN D-6585, 1972.

"Provotorov, V. P., and Riabov, V. V., "Nonsteady-State Heat Transfer upon Shock Wave Reflection in a Shock Tube," *Journal of Applied Mechanics and Technical Physics,* Vol. 28, No. 5, 1987, pp. 721–727.

[10]Ermakov, V. V., and Kalitkin, N. N., "The Optimal Step in Newton's Regularization Method," *Journal of Computational Mathematics and Mathematical Physics,* Vol. 21, No. 2, 1981, pp. 235–242.

[11]Denisenko, O. V., and Provotorov, V. P., "Study of Viscous Gas Flows in Multicomponent Mixtures," *Trudy TsAGI,* Issue 2269, 1985 (in Russian).

"Provotorov, V. P., "Improved Regularization Algorithm for Computation of the Thin-Viscous-Shock-Layer Equations," *Trudy TsAGI,* Issue 2436, 1990, pp. 165–173 (in Russian).

Charge Optimization for a Triangular-Shaped Etched Micro Heat Pipe

A. B. Duncan*
University of Illinois at Chicago, Chicago, Illinois 60607
and
G. P. Peterson†
Texas A&M University, College Station, Texas 77843

Nomenclature

$R_{c,e}$ = liquid/vapor interface radius of curvature, evaporator
$R_{\max}$ = liquidhapor interface radius of curvature, condenser
γ = liquid surface tension
ΔP_c = available capillary pressure difference
$\Delta P_{c,c}$ = condenser capillary pressure difference
$\Delta P_{c,e}$ = evaporator capillary pressure difference

Received Feb. 14, 1994; revision received Aug. 1, 1994; accepted for publication Sept. 27, 1994.

*Assistant Professor, Department of Mechanical Engineering. Member AIAA.

†Tenneco Professor and Head, Department of Mechanical Engineering. Member AIAA.

Introduction

PREVIOUS investigations have indicated that the primary transport limit occurring in micro heat pipes is the capillary pumping limit.[1] This limit occurs when the available capillary pressure difference between the evaporator and the condenser regions is not sufficient to overcome the liquid and vapor pressure drops. When the operating conditions of the heat pipe are such that the summation of the pressure losses associated with heat pipe operation exceed the available capillary pressure difference, the working fluid of the heat pipe will not be "pumped" from the condenser to the evaporator and the wicking structure will dry out. At high heat flux values, a condition may be reached where such a small amount of liquid exists in the evaporator that viscous forces in the liquid flow channel become larger than the capillary pressure difference and prohibit liquid from returning to the evaporator region. This phenomena of dryout defines the capillary wicking limit and is typically observed experimentally by either a sudden increase in evaporator temperature or a distinct decrease in effective thermal conductivity, as power input to the evaporator is increased.

Available Capillary Pressure Difference

The equation of Young and Laplace may be used to define the pressure difference between liquid and vapor phases at an arbitrarily curved interface. In order to apply this equation to the evaporator and condenser regions of a heat pipe, it must be assumed that during steady-state operation, the liquid-vapor interfaces are in a state of equilibrium with respect to the radius of curvature. It must also be assumed that mass depletion from the liquid phase in the evaporator and mass injection into the liquid phase in the condenser do not affect this equilibrium state. Historically, the equation of Young and Laplace has been used to evaluate the difference in capillary pressure between the evaporator and condenser regions in order to determine the available capillary pumping pressure for heat pipe operation as

$$\Delta P_c = \Delta P_{c,c} - \Delta P_{c,e} \tag{1}$$

When a heat pipe of triangular cross section is properly charged, a flooded condition will exist in the condenser region and the liquid-vapor interface in the condenser region will assume the shape of a hemisphere. Using a minimization of free surface energy technique,' the radius of curvature in this region can be shown to be equal to the largest radius of curvature that exists in the triangular cross section of the micro heat pipe (i.e., an inscribed circle), as illustrated in Fig. 1. For the etched micro heat pipes evaluated and tested in the current investigation, this radius of curvature $R_{c,e}$ is equal to 30.96 μm, and the equation of Young and Laplace reduces to'

$$\Delta P_{c,c} = 2\gamma/R_{\max} = 2\gamma/30.96\ \mu\text{m} \tag{2}$$

In the evaporator region, the liquid-vapor interface is initially assumed to be one dimensional (i.e., having only one nonzero radius of curvature). This assumes first, no axial variation in the radius of curvature in the evaporator, and second, that the cross-sectional radius of curvature is the same

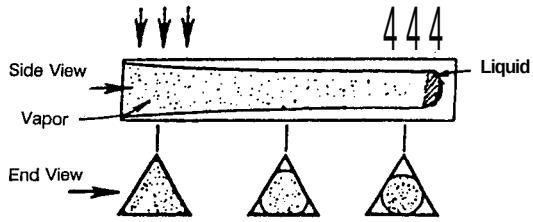

Fig. 1 Cross section of the micro heat pipe.